

# On the factors affecting strength of Portland Cement

N. B. EDEN, J. E. BAILEY

*Department of Metallurgy and Materials Technology, University of Surrey, Guildford, UK*

This paper reports mechanical property measurements for Portland Cement paste free from fabrication artifacts (e.g. bubble-type voids), and compares them to published results both for normal and new high strength cement. Removal of large voids (above 100  $\mu\text{m}$ ) by vacuum de-airing leads to an increase of  $\sim 15\%$  in mean flexural strength and a small decrease in fracture toughness. This increase in flexural strength is predictable from the tied-crack model previously proposed to explain the notch-sensitivity behaviour of hardened cement paste, and for which direct experimental evidence was obtained. It is suggested that factors such as moisture content are at least as important as large voids in controlling mechanical properties. It is concluded that the much increased strength of the new polymer-containing cements must result from improvements to the microstructure other than the simple elimination of voids.

## 1. Introduction

Recent debate about the factors controlling flexural strength of hydraulic cements [1–3] has centred around the application to them of conventional Griffith fracture criteria, and hence the steps which must be taken to improve their properties.

Higgins and Bailey [4] deduced the geometry-independent notch sensitivity curve for a cement paste of water/cement ratio 0.3 by testing a large size range of notched specimens in three-point flexure. The Dugdale model gave the best fit to this curve, predicting a yield stress of 12 MPa, which compares favourably with the unnotched flexural strength of 15 MPa deduced from the notch sensitivity curve (Fig. 10 of [4]). The process zone length was of the order of 1 mm and critical crack opening displacement 1  $\mu\text{m}$ , the values of which were confirmed by direct observation using the diffuse illumination technique [5]. Since their maximum value for tensile strength, on 10 mm  $\times$  10 mm specimens, was 12.5 MPa, remarkably close to the predicted strength, they concluded that the material was relatively insensitive to the bubble-type flaws already present.

Birchall *et al.* [1], however, produced materials from Portland Cement with flexural strengths in

excess of 60 MPa, and with overall porosity in a “similar range” to ordinary pastes. They ascribed the relatively poor performance of their normal paste to the presence of large cavities which they considered to act as sharp Griffith flaws. These were absent in the improved material and it was hence named “macro defect free” (MDF) cement. Since the original disclosure of MDF, further results have been published on such materials [6–10] and it now seems appropriate to re-assess the data for both conventional pastes and MDF preparations.

Perhaps the greatest elegance of the Griffith theory is its sound basis in thermodynamics and thus freedom from any of the empirical constants or correction factors which have continually appeared in attempts to describe mechanical behaviour, at least with regard to porous bodies.

The equation,

$$\sigma = \left( \frac{2E\gamma}{\pi c} \right)^{1/2} \quad (1)$$

where  $\sigma$  is the tensile strength of the body,  $E$  is the Young's modulus of elasticity,  $\gamma$  the surface energy and  $c$  the crack half-length, predicts an infinite strength at zero flaw size and does not, therefore, make any predictions concerning ulti-

mate strength. Furthermore, the Griffith energy balance, though necessary, is in many cases not a sufficient criterion for failure, since a mechanism must also exist for catastrophic fracture to occur. For example, if crack-blunting mechanisms exist, such as dislocation slip in ductile metals or zirconia toughening in ceramics, then the stress to fail a specimen will be higher than that calculated from Equation 1.

Birchall *et al.* [9] use the Griffith equation as a basis for the fracture of cement, inserting relationships for elastic modulus  $E$  and work of fracture  $R (= 2\gamma)$ , both empirically related to porosity. Thus a composite relationship is obtained,

$$\sigma = \left[ \frac{E_0 R_0 (1-p)^3 \exp(-dp)}{\pi c} \right]^{1/2} \quad (2)$$

where  $E_0$ ,  $R_0$  and the zero porosity values of  $E$  and  $R$ ,  $d$  is an empirical constant and  $p$  the volumetric porosity, with strength controlled by porosity and flaw size. The analysis retains the same disadvantage of infinite strength at zero flaw size, the only limit apparently being set by the yield point of the cement grains at 400 MPa [9]. Over a range of flexural strength between 60 and 150 MPa, MDF appears to have a constant calculated flaw size of approximately 100  $\mu\text{m}$  [9], even though observable cavities are in the region of only 15  $\mu\text{m}$  or less [1]. There is as yet no microstructural explanation for the origin of this apparently constant flaw size.

Assuming a flaw size of 100  $\mu\text{m}$ , and inserting the values  $E = 20 \text{ GPa}$  and  $R = 19 \text{ J m}^{-2}$  for a "normal" paste [1], a potential strength of 35 MPa is predicted. Normal hardened cement pastes containing air bubbles of the order of 1 mm diameter gave a predicted, and indeed observed, strength of around 10 MPa. Removal of the large voids (above 100  $\mu\text{m}$ ) in a cement paste, according to this simple theory should lead to a much increased strength.

It is important, however, to note the possible errors involved in the calculation. Whilst the introduction of notches into a flexural specimen of given size is known to give a reasonable fit to the Griffith equation, earlier work [4] has shown that the value of the critical stress intensity factor  $K_{Ic} (= [ER]^{1/2})$  thus obtained varies considerably with beam depth. The smallest value, for a 5 mm deep beam, was 0.33  $\text{MN m}^{-3/2}$ , rising to an extrapolated value of approximately 0.8  $\text{MN m}^{-3/2}$  for very large beams. Bailey and Higgins [2] pointed

out that since MDF cements have higher modulus of elasticity and fracture toughness, indicating an improved microstructure, they are not directly comparable with ordinary cement pastes on the basis of the Griffith flaw-size criterion alone.

On the other hand, the experimentally deduced curve of Higgins and Bailey (Fig. 10 of [4]) suggest that large improvements will not be made by removing large voids. This curve also predicts a strength of 10 MPa in the presence of 1 mm voids, but also predicts that even after removal of the voids, the strength will only rise to 15 MPa. There is a close correlation with their observed unnotched results (Fig. 3 of [4]) which lay between approximately 10 MPa and 16 MPa, the mean being around 13 MPa. Removal of the voids should, according to this model, lead to a mean strength of about 15 MPa.

In the experiments reported in this paper attempts were made to remove the large fabrication-induced voids in cement paste by means less sophisticated than the MDF process, and without appreciably changing the values of  $E$  and  $R$ , in order to monitor any effects upon strength. By comparison with similar conventional pastes which still contain relatively large cavities, such as those made by Higgins and Bailey, it is possible to examine the sensitivity of strength to these voids, independent of any arguments regarding microstructure [2, 3]. Flexural strength, Young's modulus and fracture toughness measurements were carried out.

## 2. Experimental methods

There appear to be three principal mechanisms by which fabrication voids may be formed in normal cement paste.

Firstly, inadequate compaction may result in air trapped as bubbles in the paste while it is being manipulated, either during mixing or casting. Such bubbles will form large spherical cavities which are not filled by hydration products. Size may depend principally upon surface tension, viscosity, mixing and casting techniques and any effort made to remove them.

Secondly, inadequate wetting of groups of cement grains, which are not properly dispersed into the mixing water, will cause air to be entrapped within them [9]. The size of the resulting voids will depend upon particle size and distribution of cement grains and efficiency of mixing process.

Thirdly, inadequate suspension stability will cause cement grains to flocculate after mixing, leaving large, continuous water-filled spaces in between, which may or may not later be filled with hydration products. Size will depend upon degree of freedom (space available for movement) and attraction of grains for each other.

A number of investigators [11, 12] have used evacuation at some stage in the mixing process to minimize air entrapment. Much air in bubble form can also be removed by the more common method of vibrating the mould after filling. The second class might be removed either by vigorous mixing, or by employing a wetting agent. If the cement suspension then remains stable, this should minimize the presence of the third class of void. Hardened cements free from fabrication voids were therefore made by vacuum de-airing fresh paste in a plastic desiccator at approximately 130 torr. A water/cement (*w/c*) ratio of 0.3 by weight was used.

The cement used was a typical Ordinary Portland Cement with a specific surface of  $365 \text{ m}^2 \text{ kg}^{-1}$ . Distilled water was used for mixing.

To aid thorough wetting of the cement grains, and to impart a fluid rather than plastic consistency to the paste to facilitate de-airing, 1% (by weight of dry cement) of a superplasticizer, Cormix SP1, was added to the water prior to mixing. Following the procedure of Higgins and Bailey, the constituents were mixed in a polythene bag, kneading out any lumps to ensure an even consistency. The open bag was then transferred to a plastic desiccator attached to a rotary vacuum pump.

Pressure reduction was accompanied by gentle agitation of the desiccator to burst the air bubbles which rose to the surface. A total of three cycles down to 130 torr and back to atmospheric was carried out, during which less than 1% of the water was lost by evaporation.

The resulting slurry was then poured into lightly oiled steel moulds, which were vibrated during filling, the moulds each covered with a perspex sheet and kept in a fog room overnight. After demoulding, the blocks, which measured  $200 \text{ mm} \times 50 \text{ mm} \times 30 \text{ mm}$  deep, were cured under water at  $20^\circ \text{C}$  for at least 6 weeks.

For mechanical testing, beams of the desired dimensions were cut from the blocks using a circular diamond-tipped saw, under a copious flow of water. Where required, a notch was cut in the

tension side of the beam using a 0.15 mm thick diamond saw.

All testing was done on a floor-mounted Instron universal testing machine. Crosshead speed was adjusted to keep the time to peak load within the range 15 to 30 sec, except for work of fracture tests which were all carried out at the slowest speed available,  $0.05 \text{ mm min}^{-1}$ .

To minimize flexibility in the testing machine, whilst also maintaining very high sensitivity, a Kistler piezo-electric load washer was used instead of the conventional load cell. The washer itself had a stiffness of  $6 \text{ kN } \mu\text{m}^{-1}$ , maximum load capacity of 60 kN, and the most sensitive range produced  $1 \text{ V N}^{-1}$  over the output range of  $0$  to  $\pm 10 \text{ V}$ . It was situated above the test rig, measuring the load through the loading bar rather than the support reactions.

All tests were carried out with the specimen completely submerged in water which had previously been used for curing pastes. Supports were 20 mm diameter rocking rollers which were able to roll outwards to prevent axial stresses building up in the beam.

The length/depth ratio of the principal series of three-point bend tests was kept constant at 8. To examine any size-dependence in the fracture criteria of the de-aired paste, four beam depths, 5, 10, 15, 22.5 mm were employed, with beam widths of 12 mm for the two smaller and 25 mm for the larger depths.

Young's modulus of elasticity was obtained from the flexure of a beam using the equation

$$E = \frac{kl^3}{4bd^3} \times 10^{-3} \quad (3)$$

where  $E$  is Young's modulus of elasticity (GPa),  $k$  the slope of the load-deflection plot ( $\text{N mm}^{-1}$ ),  $b$  the beam width (mm),  $d$  the beam depth (mm) and  $l$  the beam span (mm).

The error due to neglecting shear deflection is low at  $l/d = 8$ , being approximately 6% [13]. However, because of the small size of some of the specimens, and their being immersed in water, it was impractical to measure central deflection directly, and this was therefore monitored using an LVDT between the upper loading bar and the base plate holding the rollers, therefore including any crushing at the supports. Fig. 1 shows the effect of increasing the length/depth ratio to 40 for a beam depth of 5 mm, together with a calibration series of 6 mm plate glass specimens 12 mm wide, at a reduced scale.

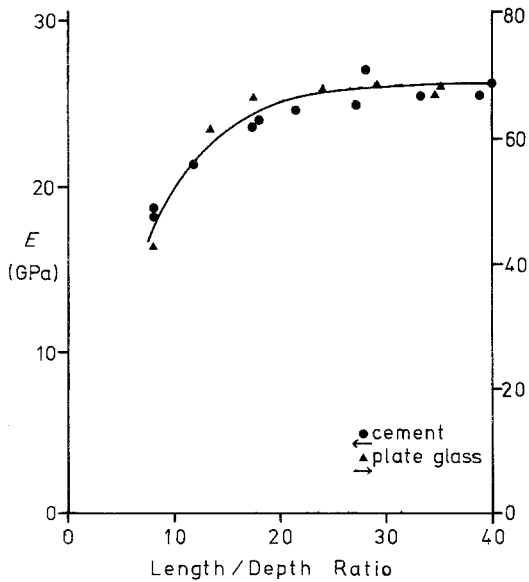


Figure 1 Effect of length/depth ratio on Young's modulus of elasticity calculated from three-point bend tests. Left-hand axis de-aired cement paste, right-hand axis soda-lime glass.

Even though the latter part of the load–deflection plot, after initial settlement, was linear up to failure for both cement and glass a marked increase in calculated modulus can be seen as  $l/d$  is raised. This is due to the stiffness of the beam reducing, as its length is increased, until it becomes very small compared to the support stiffness, and the measured value of  $E$  approaches its correct value. This was found to be 26 GPa. At  $l/d = 8$ , there was no size effect in modulus over the range of beam depths investigated in the principal series.

Flexural strength was computed from simple beam theory:

$$\sigma_f = \frac{3Pl}{2bd^2} \quad (4)$$

where  $\sigma_f$  is the flexural strength (MPa), and  $P$  the failure load (N).

A factor  $(1 - 4d/3\pi l)$  may be applied to correct for the wedging action of the point load upon the stress distribution [13], amounting to an error of approximately 5%, but is normally disregarded.

Critical stress intensity factor,  $K_{Ic}$ , was computed from the conventional equation [14]:

$$K_{Ic} = \frac{3Pla^{1/2}}{2bd^2} Y \quad (5)$$

where  $K_{Ic}$  is the critical stress intensity factor ( $MNm^{-3/2}$ ),  $a$  the notch depth (mm) and  $Y$  the polynomial geometrical factor.

A mean value was taken from six beams each at notch/depth ratios of 0.2 and 0.4. As a further test, full blocks were used to produce 30 mm wide  $\times$  200 mm long beams to be tested up to  $d = 45$  mm over a span of 180 mm, with notch/depth ratio 0.35.

Apparent fracture surface energy,  $\gamma_F$  was obtained from slow-bend specimens,  $a/d = 0.65$ , following the method of Watson [15], by integrating the load/deflection curve and allowing for the drop in potential energy of the beam.

$$\gamma_F = \frac{W + \delta w/2}{2b(d-a)} \quad (6)$$

where  $\gamma_F$  is the apparent fracture surface energy ( $Jm^{-2}$ ),  $W$  the energy under the load–deflection diagram (J),  $\delta$  the drop in centre of mass of the beam (m), and  $w$  the submerged weight of the beam (N).

At the high notch/depth ratio used, the stiffness of the beam was sufficiently low to neglect the contribution of support crushing to the indirect deflection measurement.

### 3. Results

After curing, the paste had a porosity of 34% by volume, calculated from the loss of weight on first drying from “saturated surface dry” to oven dry at  $105^\circ C$ .

Fig. 2 compares optical micrographs of polished sections of a normally compacted paste and a de-aired paste, prepared as above, both of the standard  $w/c$  ratio, 0.3. Systematic examination of such sections did not reveal any voids over  $100 \mu m$  diameter in the de-aired materials as compared to the standard sample which contained a significant number of voids of up to 1 mm diameter.

Flexural strength results are shown in Fig. 3. A marked reduction with increasing beam depth is immediately apparent, indicating a size effect in common with many other materials. Also shown in Fig. 3 are published results [4] for the same  $w/c$  ratio paste without de-airing, in three-point flexure ( $l/d = 5$ ) and the maximum strength in direct tension.

To confirm the size effect by testing a larger volume, a four-point test was carried out at a beam depth of 10 mm and span of 120 mm, the minor loading span being 40 mm. The best result is also shown in the figure, falling below any of the three-point tests as expected. Detailed comparison of the three-point, four-point and tensile tests is not

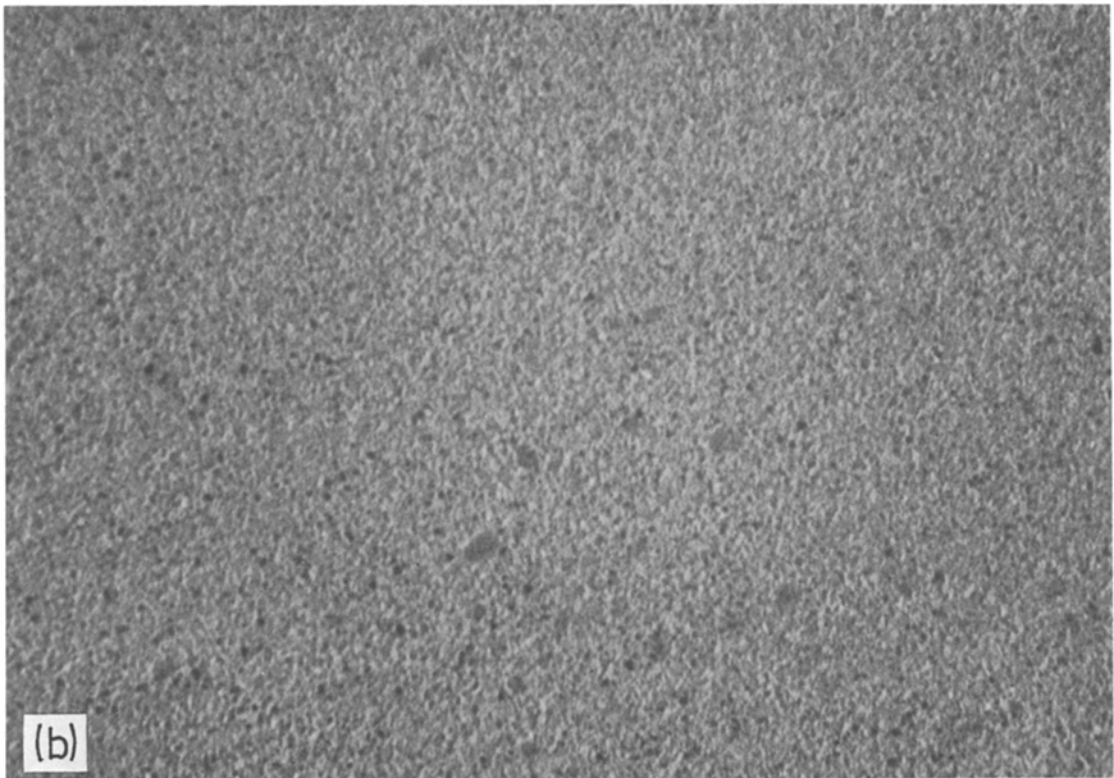
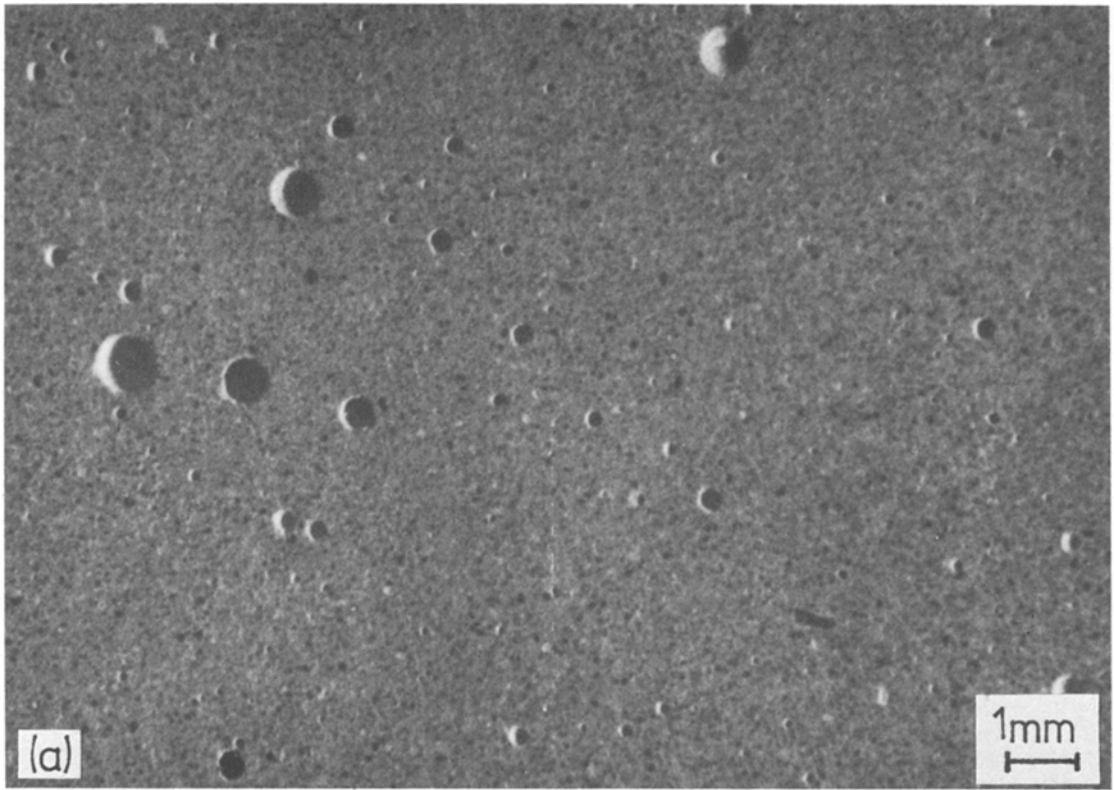


*Figure 2* Polished sections of cement pastes: (a) normal, and (b) de-aired.

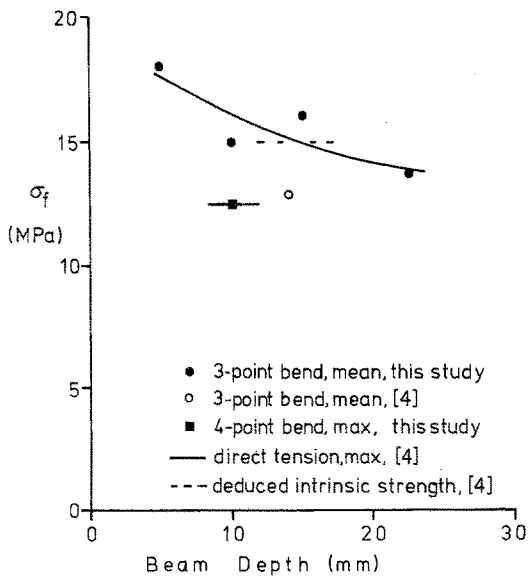


Figure 3 Effect of beam depth on measured flexural strength.

warranted in the present context because of the statistical nature of the strength dependence.

$K_{Ic}$  values are given in Fig. 4, together with the results on normally compacted pastes [4]. The result for the largest beams falls below the expected curve, and we take the meaningful value of  $K_{Ic}$  for the de-aired paste to be  $0.45 \text{ MN m}^{-3/2}$ . This is the only significant difference found between the de-aired and conventional paste. Whether it is due to the action of spherical cavities in crack-blunting, or a change in the Dugdale pro-

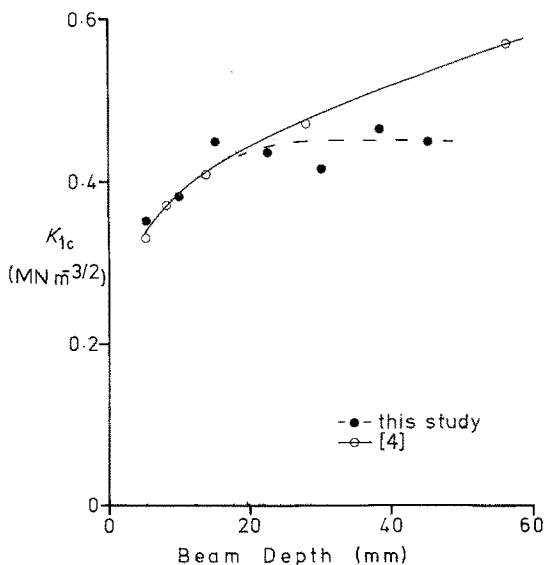


Figure 4 Effect of beam depth on measured critical stress intensity factor.

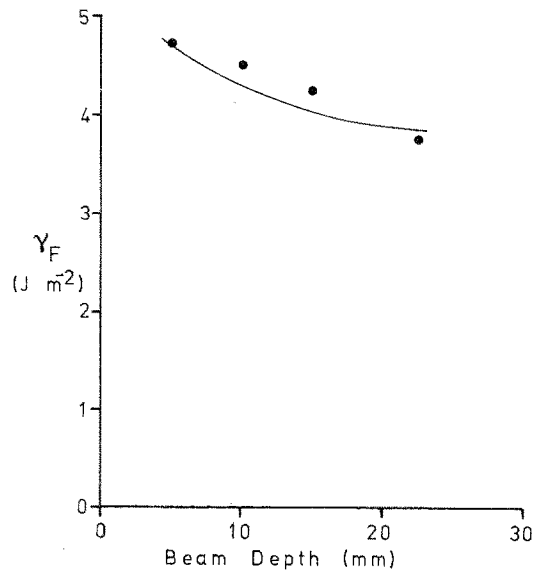


Figure 5 Effect of beam depth on measured fracture surface energy.

cess zone parameters brought about by the action or presence of the superplasticizer is not yet known.

Fig. 5 indicates that there is also a variation in  $\gamma_F$  with beam depth, though in opposition to that noted for  $K_{Ic}$ . Fig. 6 shows broken notched specimens of the four beam depths, taken under oblique lighting to highlight the surface topography. It can be seen that the increased frac-

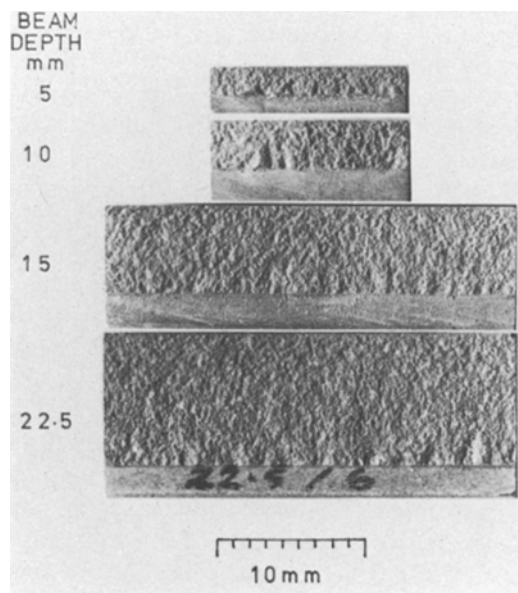


Figure 6 Crack tortuosity close to the tips of sawn notches.

ture energy in the small beams is due to crack tortuosity close to the notch tip, increasing the effective fracture area, the zone length being independent of beam depth. The line in Fig. 5 shows the computed effect of a 50% increase in effective fracture area over the first millimetre of fracture above the notch tip, with a resultant fracture surface energy of approximately  $3.8 \text{ J m}^{-2}$ .

Comparison with Watson's results [15] and those in the literature which he considered most valid indicates that this is a reasonable value for a typical cement pastes.

#### 4. Discussion

It is to be noted that the values of  $K_{1c}$  and  $\gamma_F$  considered in this study to be most valid for the de-aired paste (i.e. from large beams:  $K_{1c} = 0.45 \text{ MN m}^{-3/2}$ ,  $\gamma_F = 3.8 \text{ J m}^{-3}$ ,  $E = 26 \text{ GPa}$ ) correlate well in the equation

$$K_{1c} = (2E\gamma)^{1/2}. \quad (7)$$

Using these values it is possible to obtain a critical flaw size from the Griffith Equation, 1. Inserting  $\sigma_f = 12.5 \text{ MPa}$  (four-point bend) gives a value of  $c = 0.41 \text{ mm}$ . The highest mean strength,  $18 \text{ MPa}$  at  $d = 5 \text{ mm}$ , yields a value of  $0.2 \text{ mm}$ , though it is more logical to compare the maximum flaw size with the minimum strength. Even so, bubble defects of between  $0.2$  and  $0.4 \text{ mm}$  should be visible both on fracture surfaces and polished sections if they are responsible for generating this size of flaw. Clearly from Fig. 2 this is not the case for polished sections.

Confirmation of this discrepancy was obtained from fractography experiments. Careful study of fracture surfaces under oblique lighting, shown schematically in Fig. 7a, reveals certain directional markings. Introducing easily observed flaws by drilling small holes in the tensile face of flexural specimens, Figs. 7b and c, shows that these markings point to the origin of fracture. Examination of the fracture surfaces of many plain de-aired beams indicated that there was no obvious "flaw" at the origin of fracture. For instance, it can be seen that the beam shown in Fig. 7d failed at one corner, marked X, and SEM examination of the origin of fracture revealed no feature of similar dimensions to the flaw size of about  $400 \mu\text{m}$  calculated from the fracture toughness and failure stress. It must be concluded, therefore, that the simple Griffith equation is not a sufficient criterion to describe the fracture of Portland Cement paste.

This work does, however, support the predictions of Higgins and Bailey [4], since there is an increase in the mean strength of cement paste on de-airing of the order of 15% (from  $13$  to  $15 \text{ MPa}$ ), and furthermore the measured strength is close to the intrinsic strength deduced from the tied crack model (see Fig. 3).

An explanation is now required for the improved strength of the new polymer-containing cements. One aspect which has not been discussed in detail is the effect on measured strength of the test environment. The materials in the present study, as earlier [4], were tested under water to maintain saturation, since strength reductions have often been observed upon drying cement pastes (e.g. [16]), whereas the results both for MDF and conventional pastes quoted by Birchall *et al.* [1] and by Alford *et al.* [7] have been measured on dried specimens.

Comparison of the "normal" (dried) paste of Birchall *et al.* [1] with the present study reveals that whilst their material had lower strength ( $10.5 \text{ MPa}$ ) and modulus of elasticity ( $20 \text{ GPa}$ ) the work of fracture was considerably higher at  $R = 19 \text{ J m}^{-2}$  as compared to our de-aired wet paste (of higher  $w/c$  ratio) at  $R = 2\gamma = 7.6 \text{ J m}^{-2}$ . Furthermore, the work of fracture results of Alford *et al.* [7] on dried conventional pastes are scattered between  $19$  and  $41 \text{ J m}^{-2}$ . Similar values are also quoted for MDF preparations.

To illustrate the effect of water upon flexural strength, small beams of the de-aired paste were allowed to dry in the laboratory, after which they were tested in flexure. The flexural strength had reduced to  $10 \text{ MPa}$ . On the other hand, some of our MDF preparations, using the same cement, showed a very different behaviour, producing flexural strengths in excess of  $60 \text{ MPa}$  when dried to ambient humidity, whilst the strength was only  $24$  to  $30 \text{ MPa}$  prior to drying.

MDF and normal pastes must therefore be considered as different preparations. Whilst the strength of ordinary pastes may be limited, as suggested by Higgins and Bailey, the new MDF materials break away from this limitation by their amenability to post-curing treatment. Normal and MDF cements should not, therefore, be compared directly, as has been the practice so far, unless account is taken of this effect.

In this respect it is interesting to note that the newer forms of MDF, with strength of  $150 \text{ MPa}$ , gain this extra strength by modification of the

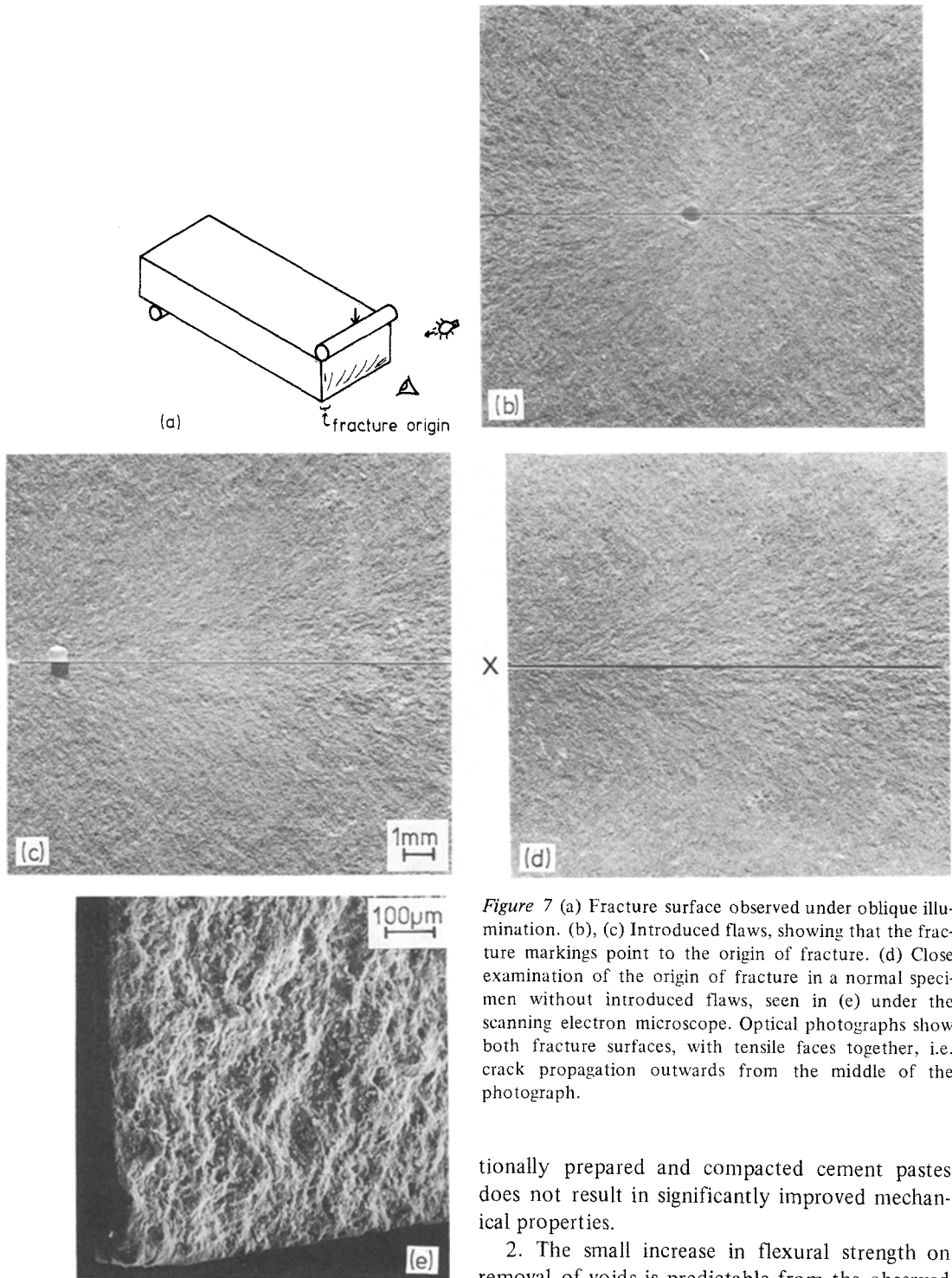


Figure 7 (a) Fracture surface observed under oblique illumination. (b), (c) Introduced flaws, showing that the fracture markings point to the origin of fracture. (d) Close examination of the origin of fracture in a normal specimen without introduced flaws, seen in (e) under the scanning electron microscope. Optical photographs show both fracture surfaces, with tensile faces together, i.e. crack propagation outwards from the middle of the photograph.

microstructure *after* initial forming [10], apparently by hot curing and oven drying [17].

## 5. Conclusions

1. Removal of air bubble defects from conven-

tionally prepared and compacted cement pastes does not result in significantly improved mechanical properties.

2. The small increase in flexural strength on removal of voids is predictable from the observed fracture mechanism in hardened cement paste.

3. A function of air bubbles in the fracture of cement may be to act as minor crack blunters or to deflect the path of a running crack.

4. Further research must be directed towards the effect of drying upon the mechanical proper-



ties of cements, especially MDF-type preparations which contain water-soluble polymers. These polymers may serve to regulate the loss of water, thus preventing drying shrinkage cracking, and even to enhance the bonding due to their adhesive capacity.

5. The enhanced strength of MDF cements must be essentially due to microstructural improvement either during or after curing.

## References

1. J. D. BIRCHALL, A. J. HOWARD and K. KENDALL, *Nature* **289** (1981) 388.
2. J. E. BAILEY and D. D. HIGGINS, *Nature* **292** (1981) 89.
3. J. D. BIRCHALL, A. J. HOWARD and K. KENDALL, *ibid.* **292** (1981) 89.
4. D. D. HIGGINS and J. E. BAILEY, *J. Mater. Sci.* **11** (1976) 1995.
5. *Idem*, Conference on Hydraulic Cement Pastes, Sheffield, Cement and Concrete Association, UK, 1976, 283–96.
6. N. McN. ALFORD, *Cem. Concr. Res.* **11** (1981) 605.
7. N. McN. ALFORD, G. W. GROVES and D. D. DOUBLE, *ibid.* **12** (1982) 349.
8. J. D. BIRCHALL, A. J. HOWARD and K. KENDALL, *J. Mater. Sci. Lett.* **1** (1982) 125.
9. *Idem*, in “Engineering with Ceramics”, Proceedings of the British Ceramic Society No. 32, edited by R. W. Davidge (1982) pp. 25–32.
10. *Idem*, *Chem. Britain* **18** (1982) 860.
11. R. A. HELMUTH and D. H. TURK, in “Structure of Portland Cement Paste and Concrete”, (SP90, Highways Research Board, 1966) pp. 135–44.
12. M. YUDENFREUND, I. ODLER and S. BRUNAUER, *Cem. Concr. Res.* **2** (1972) 313.
13. S. TIMOSHENKO, “Strength of Materials” (Van Nostrand, London, 1938).
14. N. F. BROWN and J. E. SRAWLEY, ASTM STP 410 (American Society for Testing and Materials, Philadelphia, 1967).
15. K. WATSON, *Cem. Concr. Res.* **8** (1978) 651.
16. K. M. ALEXANDER, *Nature* **183** (1959) 885.
17. J. D. BIRCHALL, A. J. HOWARD and K. KENDALL, UK Patent Application Nos. 8041640 (1980) and 8123103 (1981).

*Received 18 April  
and accepted 26 April 1983*